

SR-4000 TOF CAMERA: FURTHER EXPERIMENTAL TESTS AND FIRST APPLICATIONS TO METRIC SURVEYS

F. Chiabrando^a, D. Piatti^{b,*}, F. Rinaudo^b

^a Dept. of Human Settlements Science and Technology, Politecnico di Torino, Viale Mattioli 39,
10125 Torino, Italy
- filiberto.chiabrando@polito.it

^b Dept. of Land, Environment and Geo-Engineering, Politecnico di Torino, C.so Duca degli Abruzzi
24, 10121 Torino, Italy
- (dario.piatti, fulvio.rinaudo)@polito.it

Commission V, SS-2

KEY WORDS: ToF camera, Scattering, Object reflectivity, Angle of incidence, Accuracy, Comparison

ABSTRACT:

In recent years, a new generation of active cameras, based on the Time-of-Flight (ToF) principle, has been developed. The main advantages with respect to other 3D measurement techniques are the possibility to acquire data at video frame rates and to obtain 3D point clouds without scanning and from just one point of view. Some experimental tests relative to the calibration of the distance measurements delivered by a ToF camera (SwissRanger-4000 camera) were reported in our previous works (Chiabrando et al., 2009). Starting from those results, in this paper three main tests are described, which are all related to the SR-4000 distance measurements: the influence of the scattering artifacts caused by multiple internal reflections, the evaluation of influence of the angle between the camera optical axis and the normal to the object surface on the distance measurement precision and an investigation of the influence of object reflectivity on the camera distance measurement accuracy and precision. A comparison between SR-4000 data and LiDAR data on a real object is reported in this paper in order to show the potentiality of ToF cameras for metric survey purposes. Finally, our first experiences on the use of the SR-4000 camera for 3D object reconstruction are reported.

1. INTRODUCTION

Time of Flight cameras are usually characterized by no more than a few thousands of tens of pixels, a maximum unambiguous measurement range up to thirty meters and small dimensions. These devices deliver a range image and an amplitude image with infrared modulation intensities at video frame rates: the range image (or depth image) contains for each pixel the radial measured distance between the considered pixel and its projection on the observed object, while the amplitude image contains for each pixel the strength of the reflected signal by the object.

As reported in different works (Lindner & Kolb, 2006; Falie & Buzuloiu, 2007) and in our previous tests (Chiabrando et al. 2009) the distance measurements of ToF cameras are influenced by some systematic errors. In order to model these errors we proposed a distance error model for the SwissRanger-4000 camera, which is unique for all the camera pixels and which can be applied to data acquired with the standard software supplied with the camera.

In the following sections, further experimental tests on the SR-4000 distance measurements are reported. In particular, three main aspects are treated. First, in section 2 the influence of the scattering artifacts caused by multiple internal reflections on the distance measurement accuracy is analyzed. Then, the evaluation of influence of the angle between the camera optical axis and the normal to the object surface on the distance measurement precision is investigated in Section 3. The third aspect (section 4) deals with a systematic investigation of the

influence of object reflectivity on both camera distance measurement accuracy and precision. Finally, a comparison between SR-4000 data and LiDAR data on a real object is reported in order to show the potentiality of ToF cameras for applications such as metric surveys and 3D object reconstruction.

2. INFLUENCE OF SCATTERING ON DISTANCE MEASUREMENTS

Previous works have reported that the SR-3000 line of sensor is affected by the scattering artifacts caused by multiple internal reflections occurring inside the camera, which significantly limited its distance measurement accuracy (Mure-Dubois & Hugli, 2007; Kavli et al., 2009). This effect, also called "internal superimposition", originates when some incoming signals are reflected in the camera itself, overlaying the directly reflected incoming signals on their way to the pixel. Consequently, the stronger direct signal is changed in phase (and amplitude) by the reflecting parts belonging to neighboring pixels, generating an error in the distance measurements. Usually, the scattering effect is non-local and light from a single point in the image will affect a large area of the image and will be added to the focused light received at each pixel. Since the scattered light usually originates from objects in the scene that are at different distances, the signal will have different phase shifts, which introduce an error in the measured distance. In (Mure-Dubois & Hugli, 2007) and (Kavli et al., 2008) some particular procedures from image restoration have been

* Corresponding author

proposed in order to partially correct this effect. In particular, in (Kavli et al., 2008) an average reduction of the error by more than 60% is obtained, but errors of some centimeters still remain.

In order to verify if the SR-4000 camera measurements are influenced by the scattering artifacts too, the following procedure was performed.

The camera was positioned on a photographic tripod, parallel to a wall of our laboratory. The distance between camera and wall was 2.491 m. A Plexiglas panel covered with white sheet was positioned on a total station and interposed between the 3D camera and the wall (Figure 1).



Figure 1. System adopted to study the influence of “scattering” on the camera distance measurements.

After the camera warm up, 50 frames were acquired using the “auto integration time” suggested by the SR_3D_View software for each of the following cases: wall without the panel and panel between camera and wall at 5 different distances (Table 1). The distances between the wall and the panel were measured with the total station. In order to reduce the measurement noise, the 50 frames were averaged for each case.

Case [-]	Integration time [ms]	Distance between wall and panel [m]	Distance between camera and panel [m]
WALL	150	no panel	2.491
A	150	0.517	1.974
B	111	0.760	1.731
C	75	1.017	1.474
D	52	1.264	1.227
E	34	1.514	0.977

Table 1. Data acquisition information.

A representation of an horizontal cross-section of the averaged point clouds is reported in Figure 2. As one can observe, little variations of the distance data on the wall are present, except for the image borders, where the measurements are more noisy. In order to quantitatively evaluate how much the scattering effect influence the camera distance measurements, the differences between the range image of the wall without the panel (named “WALL” in Table 1) and the range images with the panel at different distances were calculated. The results are represented in Figure 3, where the notation “W-N” indicates the difference between the range image of the wall (W) and the range image of the n-th case (N).

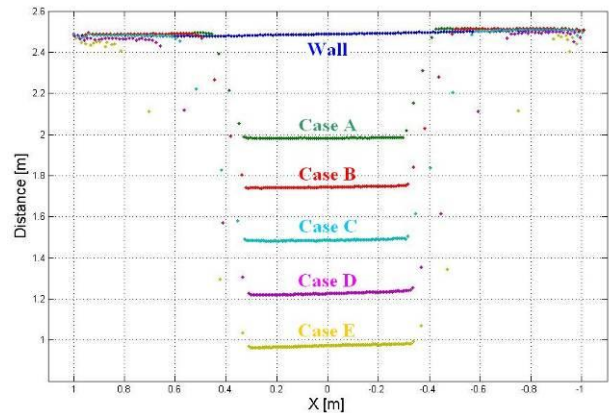


Figure 2. Horizontal cross-section (centred with respect to the sensor) of the averaged point clouds.

The analysis was limited to the area of the wall which was visible in each case (it is roughly represented in blue colour in Figure 3 for each case). In those areas, the mean value of the differences between the range images was estimated (Figure 3) and resulted of the same order of the SR-4000 distance measurement accuracy.

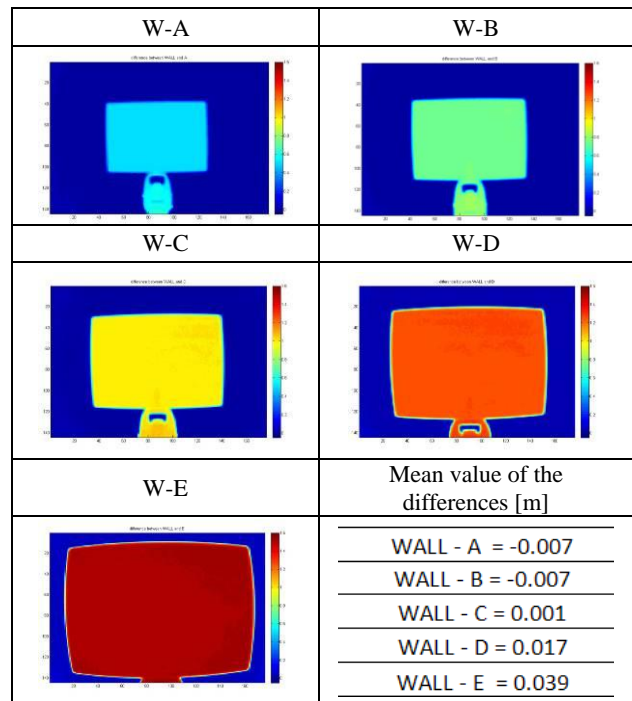


Figure 3. Range images of the differences between W and the range image of the n-th case (N) (arbitrary color scale).

In case “WALL-E”, the mean value of the differences is bigger with respect to the other cases. This fact is justified by the following considerations. Since in this case the camera and the panel are quite close to each other and the area of analysis is very small, the analysis is relative to the image borders, where the distance measurements are noisier and less accurate because of the lower signal amplitude with respect to the central part of the image. Moreover, the “auto integration time” adopted in this case is smaller than in the other cases, consequently the signal reflected by the wall is weaker and the distance measurements are noisier and less accurate.

In order to verify these considerations, the aforementioned data processing was repeated limiting the analysis area to the same border area for all the five cases: the results are practically the same of Figure 3 (bottom right). This means that the larger mean value of case “WALL-E” is mainly related to the smaller adopted integration time and the closer distance between camera and panel with respect to the other cases, which drastically reduced the amplitude of the reflected signal from the wall.

In conclusion, the SR-4000 distance measurements are not affected by the scattering artifacts caused by the presence of objects positioned at different distances in the scene.

3. INFLUENCE OF ANGLE OF INCIDENCE ON DISTANCE MEASUREMENTS

The signal emitted by the camera impinges the observed object with an angle which depends on the camera orientation with respect to the normal of the object surface. We can define alpha as the angle between the camera optical axis and the normal to the object surface, as shown in Figure 4.

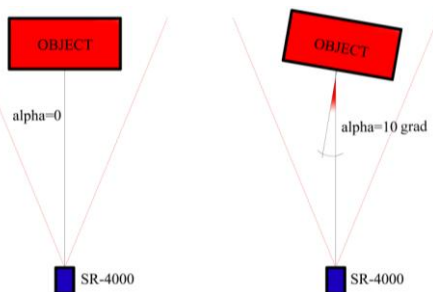


Figure 4. Alpha angle between camera optical axis and the normal to the object surface.

Some previous works have already examined the influence of the emitted signal angle of incidence on distance measurement precision (Anderson et al., 2005; Kavli et al., 2008). In the present work we analyze this aspect from a more practical point of view: our analysis deals with data acquired with the SR_3D_View software using the “auto integration time”, so changing the integration time for each object position as a generic user could do acquiring data of the object to be surveyed.

In order to evaluate if there is an influence of the alpha angle on the precision of distance measurements acquired in this way, the following system was set up.

The camera was positioned on a photographic tripod, with the camera front parallel to a Plexiglas panel, which was fixed to a Leica TS (Figure 5); the panel was covered with white sheet. After the camera warm up, using the Leica TS, the panel was accurately rotated each two grad in the 0 ÷ 50 grad rotation interval, both in clockwise direction and counterclockwise direction, while the SR-4000 camera was fixed. Fifty consecutive frames were acquired for each panel position, using an integration time equal to the “auto integration time” suggested by the SR_3D_View software. The distance between the panel and the camera was about 1.6 m.

In order to accurately estimate the distribution of the distance measurements around their mean value, a reference plain for each panel position was estimated after outlier elimination from the acquired range images thanks to a robust estimator, the Least Median Squares (LMS) estimator (Rousseeuw & Leroy, 1987).



Figure 5. System used to evaluate the influence of the alpha angle on camera distance measurements.

This estimator has a high breakdown point, which means that it can discriminate outliers and leverage points up to a percentage of 50% of the considered data. The parameter which has more influence on the LMS results is the threshold value of rejection L, that represents a preliminary hypothesis on the percentage of outlier contamination. After testing this estimator on several randomly generated range images containing different percentages of outliers, we adopted a threshold value of rejection $L = 1.5$.

The LMS estimator was applied on a sub-image of 65×61 pixel dimensions, which was centred with respect to the panel centre in each position. Thanks to this estimator it was possible to select some reliable points into the sub-image which were necessary for a robust plain estimation. Then the differences between the range image (obtained after averaging fifty frames) and the estimated reference plain were calculated for each panel position, always considering the sub-image of 65×61 pixel dimensions. The mean and standard deviation values of that differences are reported in Figures 6 and 7 respectively. In the case of alpha angles larger than fifty grad the area of the panel was too small for a reliable estimation of a reference plain, so our analysis was limited to fifty grad in both directions.

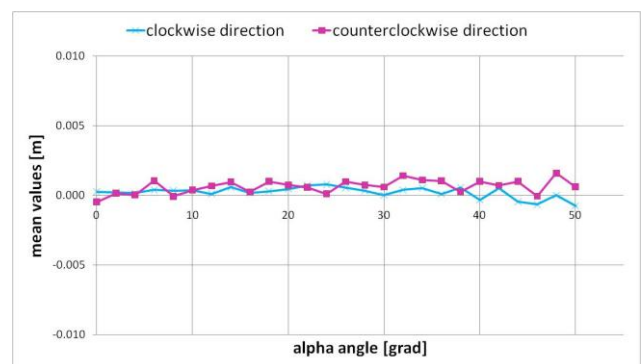


Figure 6. Mean values of the differences between range image and estimated reference plain.

From Figure 6 one can observe that the mean value of the differences between the estimated plain and the SR-4000 distance measurements shows small fluctuations around the zero value according to the alpha angle: these small fluctuations are limited to about 2 mm in both clockwise and counterclockwise directions. Instead, the standard deviation value varies according to the alpha angle (Figure 7): this variation is contained in about 2 mm. This trend is justified by the adopted procedure: since the data were acquired with the “auto integration time” for each panel position, the reduction of the amount of reflected light from the panel is limited to about 20%

with respect to the reflected light from the initial position (alpha angle equal to zero). The distance measurement standard deviation is in inverse proportion with respect to the amplitude of the reflected light (Büttgen et al., 2005; Steiger et al., 2008; Blanc et al., 2004); therefore, an amplitude reduction of about 20% will approximately result in an increment of about 25% of the distance measurement standard deviation. Since the typical standard deviation value of the distance measurements is 4 mm (www.mesaimaging.com), a 25% increment of that value is negligible. This aspect is confirmed by the afore reported results. In conclusion, adopting the “auto integration time” for data acquisition, there is no appreciable variation of the distance measurement precision for camera orientations included within the considered alpha angle interval.

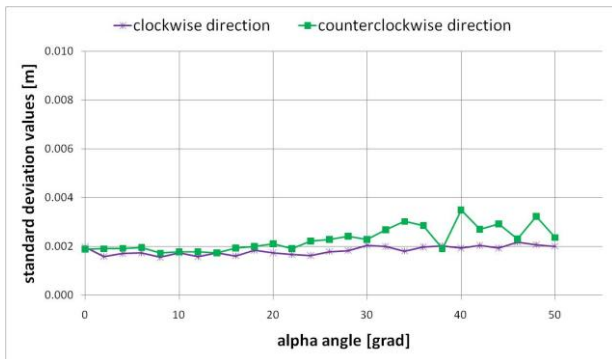


Figure 7 – Standard deviation values of the differences between range image and estimated reference plain.

4. INFLUENCE OF OBJECT REFLECTIVITY ON DISTANCE MEASUREMENTS

As already mentioned before, the distance measurement standard deviation is in inverse proportion with respect to the amplitude of the reflected light, which in turn depends on the object reflectivity to the camera emitted signal if all the other parameters (integration time, distance between camera and object, background illumination) are kept constant. Therefore, a study of the influence of object reflectivity on the SR-4000 distance measurements is necessary in order to better investigate the camera potentiality for metric surveys. For this purpose, the system represented in Figure 8 was realized.



Figure 8. Purpose-built system for positioning planar objects of different dimensions.

It allows to position planar objects of different dimensions to be tested, with high stability with respect to displacements induced by changing the objects thanks to appropriate supports. The camera was positioned on a photographic tripod, parallel to the wooden panel of the system.

Before data acquisition, a camera warm up of 40 minutes was performed. The materials to be tested were positioned from time to time on the system, while the camera was always in the same position. For each material 50 frames were acquired and then averaged in order to reduce the measurement noise. This procedure was repeated for several distances (from 1.30 m to 1.80 m) between the camera and the tested objects, moving the camera with respect to the system.

The camera positions (5 points for each position) and the object surface positions (6 points for each object and for each camera position) were estimated in an arbitrary coordinate system thanks to accurate topographic measurements using two total stations (Figure 9).



Figure 9. Topographic measurements for the estimation of camera and tested object positions.

The tested materials and the integration times (I.T.) adopted for data acquisition in the considered case (1.799 m of distance from the camera) are reported in Table 2: the tested planar objects were chosen among common materials which could be found in the case of both indoor scene reconstruction and architectural element survey.

Distance between camera and tested object surface: 1.799 m		
Material [-]	I. T. auto [ms]	I.T. ref. [ms]
Kodak R27 dark	106	106
Kodak R27 bright	102	106
Hardboard	107	106
Black paper	107	106
Laminated wood	105	106
Bright plasterboard	104	106
Painted metal sheet	99	106
Marble Pietra Etrusca	108	106
Balmoral Red Granite	107	106
Granite	107	106
Marble Pietra Orsera	105	106
Stone	107	106

Table 2. Results considering data acquired with the “I.T. auto” (1.799 m).

In the following, only the data acquisition and processing details relative to a distance of 1.799 m between camera and system are reported. For each material the 50 frames were acquired twice, with different integration times: with the “I.T. auto” (“auto integration time”), which shows little variations

depending on the material reflectivity; with “I.T. ref.”, which corresponds to the “auto integration time” for Kodak R27 grey card, that was adopted as reference integration time for the considered distance. In this way, it is possible to compare the reflectivity of the tested materials with respect to the “standard reflectivity” obtained for the Kodak R27 grey card.

In order to avoid noise effects caused by the presence of the wooden panel and of the depth discontinuity between the wooden panel and the surface to be tested, the analysis of the SR-4000 distance measurements was limited to a square area internal to the surface of the tested materials. For each of them, the differences between the estimated plain (using the points acquired with the topographic survey) and the camera distance measurements were estimated, considering both the “I.T. auto” and the “I.T. ref.”. The mean and standard deviation values of the differences for “I.T. auto” are reported in Table 3. Similar results have been obtained for “I.T. ref.”. Moreover, the following information about the acquired data in the area of analysis are reported in Table 3: the mean precision, which is the mean value of the distance measurement precision calculated as standard deviation of the 50 measurements for each pixel; the mean value of the amplitude image; the percentage of saturated pixels in the area of analysis.

From Table 3 one can observe that the mean value of the calculated differences shows small variations considering the tested materials, which are of the same order of the camera distance measurement accuracy. It is worth nothing that the mean value of the differences (raw data accuracy) of all the considered materials is 3 mm, accordingly to the measurement accuracy estimation performed in (Chiabrando et al., 2009); the same variations were observed using “I.T. ref.”. The standard deviation value of the calculated differences is less than 2 mm for all the materials, except for “Balmoral Red Granite”, “Antigorio Scuro” and “Marble Pietra Orsera”. For these materials, in fact, there was a high percentage of saturated pixels due to their high reflectivity to the camera signal and the distance measurements were quite heterogeneous.

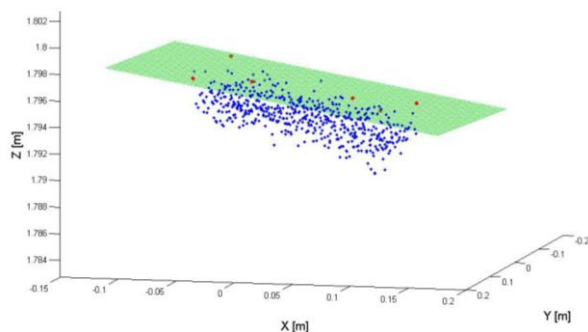


Figure 10. 3D representation of the SR-4000 point cloud obtained from averaging the acquired frames (blu dots) and the estimated plain (green) in the area of analysis. The red dots represent the topographic points used for the plain estimation.

Moreover, the mean value of the estimated distance measurement precision shows appreciable variations considering different materials: for instance, it duplicates considering the “Kodak R27 dark” (0.005 m) instead of the “Kodak R27 bright” (0.002 m) since the amplitude of the reflected signal halves. However, the worse measurement precision of 0.005 m obtained for some materials is still acceptable for our applications. In Figure 10 a 3D representation of the SR-4000 point cloud obtained from averaging the acquired frames (blue dots) and the estimated plain (green) in the area of analysis is reported for the “Kodak

R27 dark”. The red dots represent the topographic points used for the plain estimation.

5. OBJECT SURVEY AND COMPARISON

In order to investigate the actual applicability of ToF cameras for the metric survey of real objects and architectural elements, some data of an architectural frieze were acquired with the SR-4000 camera in our laboratory.

As shown in Figure 11, the frieze was positioned on a table, in front of the SR-4000 camera at a medium distance of 2 m. Seven purpose-built cubic targets covered with white sheet were distributed around the object to be acquired in order to have reference points to be exploited for comparing the ToF camera data with the LiDAR data. Fifty frames were acquired with the SR-4000 camera and then averaged in order to reduce the measurement noise. Then, the Mensi S10 laser scanner was employed to acquired data of the frieze (Figure 11 right), with a medium step of 2 mm and sub-millimetric precision.



Figure 11. Data acquisition of a frieze with the SR-4000 camera and the Riegl Mensi S10 laser scanner.

Several points were selected on both the SR-4000 point cloud and the Mensi S10 point cloud in order to have all the data in the same coordinate system. In the case of the SR-4000 data, the Z coordinate (orthogonal distance between the camera front and the object) of the selected points was corrected with the distance calibration model proposed in (Chiabrando et al., 2009) in order to obtain more reliable coordinates for the spatial similarity transformation.

Since the Mensi S10 laser scanner has a sub-millimetric accuracy, the data acquired with this instrument can be used as reference data for the SR-4000 measurement accuracy estimation on real objects. Therefore, the difference between the distance of the corresponding point on the Mensi S10 data (reference data) and the distance measured by each pixel of the SR-4000 camera was calculated (ToF original data).

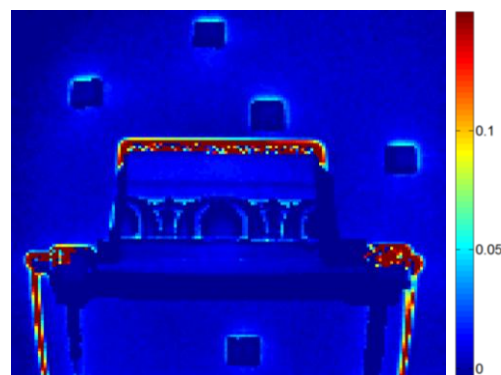


Figure 12. Differences between distances obtained from the Mensi S10 point cloud and the SR-4000 point cloud.

Figure 12 shows that the estimated differences vary considering objects which are at different distances from the camera since the error function depends on the distance between camera and object. Since the SR-4000 data and the Mensi S10 data were acquired from slightly different viewpoints, some areas in Figure 12 show high difference values which are wrong. The mean value of the differences in the frieze area considering the original ToF data is 0.006 m, while applying the proposed distance calibration model, the mean value of the differences become 0.001 m. These results demonstrate the efficacy of the previous proposed model and show the high potentiality of ToF cameras for metric surveys of architectural artifacts and for 3D object reconstruction.

6. CONCLUSIONS AND FUTURE WORKS

In this work some tests relative to the distance measurements of the SR-4000 ToF camera have been reported. The results show that the SR-4000 distance measurements are not affected by the scattering artifacts caused by the presence of objects positioned at different distances in the observed scene. Then, we demonstrated that adopting the “auto integration time” for data acquisition, there is no appreciable variation of the distance measurement precision for camera orientations included within the considered alpha angle interval with respect to the object surface normal. Besides, a systematic investigation of the influence of object reflectivity on the camera distance measurement accuracy and precision was performed, which outlined that the object reflectivity strongly influence the distance measurement precision. However, the worse measurement precision of 0.005 m obtained for some of the tested materials is still acceptable for our applications. Finally, thanks to a comparison between SR-4000 data and LiDAR data on an architectural element, we demonstrated the high potentiality of ToF cameras for metric surveys of architectural elements and for 3D object reconstruction. Future works will try to register ToF data acquired from different positions and to obtain metrically correct 3D models. In Figure 13 an example of our first experiences on 3D object modeling is reported.



Figure 13. ToF Point cloud (left), mesh (centre), textured final model (right).

REFERENCES

- Anderson, D., Herman, H., Kelly, A., 2005. Experimental characterization of commercial flash lidar devices. In: *Proceedings of International Conference on Sensing Technologies*, Palmerston North, New Zealand.
- Blanc, N., Oggier, T., Gruener, G., Weingarten, J., Codourey, A., Seitz, P., 2004. Miniaturized smart cameras for 3D-imaging in real-time. In: *Proceedings of IEEE Sensors*, Vienna, Austria, pp. 471-474.
- Büttgen, B., Oggier, T., Lehmann, M., 2005. CCD/CMOS Lock-in pixel for range imaging: challenges, limitations and state-of-the-art. In: *Proceedings of 1st Range Imaging Research Day*, Zurich, Switzerland, pp. 21-32.
- Chiabrando, F., Chiabrando, R., Piatti, D., Rinaudo, F., 2009. Sensors for 3D Imaging: Metric Evaluation and Calibration of a CCD/CMOS Time-of-Flight Camera. *Sensors*, 9, pp. 10080-10096.
- Falje, D., Buzuloiu, V., 2007. Noise characteristics of 3D Time-of-Flight cameras. In: *Proceedings of IEEE Symposium on Signals Circuits & Systems (ISSCS)*, Iasi, Romania, pp. 229-232.
- Kavli, T., Kirkhus, T., Thielmann, J., Jagielski, B., 2008. Modeling and compensating measurement errors caused by scattering Time-Of-Flight cameras. In: *Proceedings of SPIE, Two-and Three-Dimensional Methods for Inspection and Metrology VI*, San Diego, CA, USA.
- Lindner, M., Kolb, A., 2006. Lateral and depth calibration of PMD-distance sensors. In: *Proceedings of ISVC*, Lake Tahoe, NV, USA, pp. 524-533.
- Mure-Dubois, J., Hugli, H., 2007. Real-Time Scattering compensation for Time-of-Flight camera. In: *Proceedings of ICVS*, Bielefeld, Germany, pp. 117-122.
- Rousseeuw, P.J., Leroy, A.M., 1987. Robust Regression and Outlier Detection. *Wiley Series in Probability and Mathematical Statistics*, Wiley, New York, NY, USA.
- Steiger, O., Felder, J., Weiss, S., 2008. Calibration of Time-of-Flight range imaging cameras. In: *Proceedings of the 15th IEEE ICIP*, San Diego, CA, USA, pp. 1968-1971.
- www.mesa-imaging.ch (accessed on March 2010).

I.T. AUTO - Distance between camera and tested object surface: 1.799 m					
Material [-]	Mean of the differences [m]	Std of the differences [m]	Mean precision [m]	Mean amplitude [-]	% saturated pixels [%]
Kodak R27 dark	0.002	0.001	0.005	2208	0
Kodak R27 bright	0.001	0.001	0.002	6751	0
Hardboard	0.002	0.001	0.003	5113	0
Black paper	0.001	0.001	0.004	3328	0
Laminated wood	0.006	0.001	0.002	6513	0
Bright plasterboard	0.001	0.001	0.002	6808	0
Painted metal sheet	0.008	0.001	0.002	8263	0
Marble Pietra Etrusca	0.002	0.001	0.004	3003	0
Balmoral Red Granite	0.003	0.721	0.004	3322	14
Antigorio Scuro	0.004	0.781	0.003	3971	16
Marble Pietra Orsera	0.007	0.739	0.005	6513	14
Stone	0.000	0.001	0.005	2406	0
Mean value for all the materials	0.003	0.187	0.003		

Table 3. Results considering data acquired with the “I.T. auto” (1.799 m)